

## Suppression of chaos in weakly coupled diode resonators

Jong Cheol Shin and Sook-II Kwun

*Department of Physics, Seoul National University, Seoul 151-742, Korea*

Youngtae Kim

*Department of Physics, Ajou University, Suwon, Kyunggi-Do 441-749, Korea*

(Received 4 January 1993)

We have demonstrated through the system of two coupled driven diode resonators that chaos of the diode resonators can be reduced by weak coupling. Stable periodic orbits emerge from the chaotic attractor when a small coupling signal perturbs the diode resonator. However, we find that the stability of the periodic orbits is strongly dependent on the coupling signals. Our results are examined with recently proposed techniques for controlling chaos.

PACS number(s): 05.45.+b

### I. INTRODUCTION

Chaos can be commonly found in nature. By the inherent nature of long-term unpredictability, chaotic motions have been generally regarded as undesirable in many systems even though they sometimes improve system performances such as mixing or combustion efficiency. Therefore the control or suppression of chaos is of much practical importance but it has received little scientific attention until Ott, Grebogi, and Yorke (OGY) proposed a method of controlling chaos [1]. The key idea of the OGY method is the following: A chaotic attractor consists of an infinite number of embedded unstable periodic orbits. By applying small carefully chosen time-dependent perturbations to the chaotic system, the chaotic attractor can be stabilized into one of the embedded periodic orbits. They have concluded that the chaotic systems have more flexibility because their method provides a way to create a large variety of periodic motions from the chaotic system.

According to the recent experimental results, the OGY method has been proved to be efficient in many physical systems. For example, periodic orbits from the chaotic attractor of a driven magnetoelastic ribbon [2] and from the chaotic flows in a thermal convection loop [3] have been stabilized experimentally by applying small perturbations to the system control parameter. A generalized OGY method has also been introduced to handle high-dimensional systems and this method needs no knowledge of the underlying dynamical equations [4]. Another interesting method of controlling chaos is to apply weak periodic modulations to the system control parameter [5]. It has been demonstrated that the chaotic motion can be converted into a periodic one when it becomes phase-locked to the external periodic modulation by the nonlinear resonant parametric amplification studied earlier by many authors [6–8]. Chaos of the spin-wave instability in a yttrium-iron-garnet oscillator has been successfully stabilized into periodic motions by implementing this method [9].

In this paper, we report the stabilization of the unsta-

ble periodic orbits embedded in the chaotic attractor of a driven diode resonator by weak coupling to another diode resonator. Power spectra and return maps of the time signals of the coupled diode resonator clearly indicate that the chaotic attractor is reduced into a variety of periodic orbits, sometimes with period 16, when the appropriate coupling is made. Our experiments suggest that the coupled systems having the same dynamical property such as period doubling are efficient in suppressing chaos. However, stabilizing specific periodic orbits by the weak coupling, thus controlling chaos, seems to be much more intricate. The relation between our results and the recent techniques of controlling chaos is examined.

### II. EXPERIMENTS AND RESULTS

The system used in our experiments consists of two diode resonators which are coupled inductively to each other. Each diode resonator has a resistor  $R$  (100  $\Omega$ ), an inductor  $L$  (10 mH), a small-signal silicone  $p$ - $n$  junction diode (1N4007), and a coupling inductor  $L'$ , and all components are connected in series as shown in Fig. 1. Inductive coupling of the two resonators is made through the coupling inductors which are solenoids wrapped around a common ferrite cylinder. By removing the coupling inductor we can have two uncoupled resonators. To achieve the weak coupling between the resonators' self-inductance  $L'$  and mutual inductance  $M$  are made to be less than 5% of the main inductance  $L$ . Sinusoidal driving voltages  $V_1$  and  $V_2$  are supplied by a signal generator (HP 3325B) through two potentiometers. Therefore,  $V_1$  and  $V_2$  can be changed independently by varying the resistance of the potentiometers. The frequency  $f$  of the driving signal is set to 100 kHz which is near the resonance frequency of the resonators.

We observe that the uncoupled resonators show the expected period-doubling and period-adding bifurcations which are typical for a single diode resonator [10]. [See Fig. 2(b).] The motion of each resonator is observed through the time signals, the corresponding power spec-

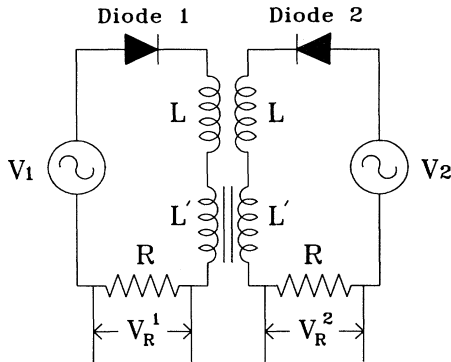


FIG. 1. Schematic circuit diagram of weakly coupled diode resonators.  $L'$  is a coupling inductor of solenoid type.  $R = 100 \Omega$  and  $L = 10 \text{ mH}$ . 1N4007 silicone  $p$ - $n$  junction diodes are used for diode 1 and diode 2.

tra, and the Poincaré sections (or return maps) of the voltage across the resistor  $R_1$  or  $R_2$  by increasing the drive signal  $V_1$  or  $V_2$ , respectively. For the coupled resonators a large variety of signals of the resonator with diode 1 (which will be called a “drive” system) by varying  $V_1$  can be applied to the resonator with diode 2 (which

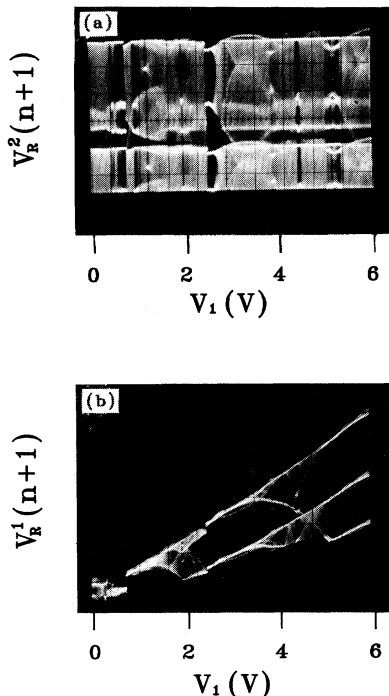


FIG. 2. (a) A bifurcation diagram showing the change of chaos of the response system at  $V_2 = 4.25 \text{ V}$  as a function of  $V_1$  of the drive system.  $V_1$  is varied from 0 to 6.0 V. Note that various periodic orbits from the chaotic attractor are emerged in several regions of  $V_1$ . Arbitrary units are used for the vertical axis. (b) A bifurcation diagram of the drive system for the same range of  $V_1$  ( $V_2 = 4.25 \text{ V}$ ). Because of the weak coupling the diagram is very similar to that of the uncoupled resonator. Arbitrary units are used for the vertical axis.

will be called a “response” system) through the coupling inductors.

Our experimental method of suppressing chaos is the following: We choose a chaotic attractor by varying  $V_2$  of the response system when  $V_1 = 0 \text{ V}$ . In the experiments we choose three chaotic attractors at  $V_2 = 1.80, 4.25, \text{ and } 9.80 \text{ V}$ . The chaotic attractor at  $V_2 = 1.80 \text{ V}$  looks very similar to that of the logistic map and this suggests that the attractor is low dimensional. The chaotic attractor at higher  $V_2$  has a fractal shape with stretchings and foldings, indicating that it is a high-dimensional attractor. Leaving the response system in a chaotic state, various weak-coupling signals are applied to the response system by increasing  $V_1$ . The time series and the return maps of the voltage across the resistor  $R_2$  are observed to see the change of the chaotic motion of the response system. The time-series data recorded by a digital storage oscilloscope (Nicolet 630) are processed to get the corresponding power spectra using an internal fast-Fourier-transform (FFT) analyzer. To test whether the coupling strength is weak, we also measure a bifurcation diagram of the resistor voltage  $V_R^1$  of the drive system.

Following our method we observe that various periodic orbits embedded in the chaotic attractor are stabilized from the chaotic response system. Figure 2(a) is a bifurcation diagram of the resistor voltage  $V_R^2$  of the response system as a function of  $V_1$  of the drive system. The amplitude  $V_2$  is 4.25 V and  $V_1$  is varied from 0 to 6.0 V. The horizontal and vertical axes represent the amplitude of drive signal  $V_1$  and peak values of the voltage signal  $V_R^2$  of the response system, respectively. The figure clearly shows that the initial one-band chaotic orbit at  $V_2 = 4.25 \text{ V}$  and  $V_1 = 0 \text{ V}$  is suppressed at several regions of  $V_1$  and various periodic orbits are retrieved as well when the appropriate perturbations signal from the drive system are introduced. Introduction of the small perturbations does not always guarantee the suppression of chaos. We find that the weak coupling often has no effect, so most of the region in Fig. 2(a) still remains chaotic. Figure 2(b) is a bifurcation diagram of the resistor voltage  $V_R^1$  of the drive system for the same range of  $V_1$  in the presence of the coupling with the response system at  $V_2 = 4.25 \text{ V}$ . Because of the weak coupling, the observed bifurcation diagram is very similar to that of an uncoupled resonator although the coupling signal from the response system also perturbs the drive system.

We observe the interesting result that periodic orbits can also be generated in the chaotic response system even though chaotic coupling signals of the drive system are introduced. For example, we see a very narrow region of the period-5 orbit around  $V_1 = 1.86 \text{ V}$  in Fig. 2(a). Because of the coupling the drive system is also locked to the period-5 orbit as shown in Fig. 2(b) but  $V_1 \approx 1.86 \text{ V}$  is actually located in the chaotic region of the uncoupled resonator. The chaotic coupling signal from the drive system reduces chaos of the response system into a periodic motion and then the periodic signal makes the drive system periodic by feedback. This is an unexpected result compared to the OGY method which uses carefully chosen time-dependent perturbation signals. However,

Fig. 2 shows that periodic signals are more efficient in suppressing chaos than chaotic signals.

In Fig. 3, we show the return map and the power spectrum of the stabilized orbit of period 4 at  $V_1=2.50$  V and  $V_2=4.25$  V. Figure 3(a) is a double exposure of the four overexposed dots of the period-4 orbit with the return map of the chaotic attractor of the uncoupled resonator ( $V_1=0$  V and  $V_2=4.25$  V). The dots of the periodic orbit are deviated very slightly from the chaotic attractor supporting the fact that a chaotic attractor consists of an infinite number of unstable periodic orbits. Figure 3(b) is the corresponding power spectrum obtained from the time series of the stabilized orbit. It clearly shows the sharp peaks at every multiple of  $f/4$  ( $f=100$  kHz), which indicates that the stabilized motion is strongly periodic. Figures 4(a) and 4(b) are the return map with the double-exposed chaotic attractor and the corresponding power spectrum of a stabilized period-5 orbit at  $V_1=1.86$  V and  $V_2=4.25$  V, respectively. Since the coupled signal for Fig. 4 is weaker than that for Fig. 3, the dots of the period-5 orbit are almost on the chaotic attractor. The power spectrum in Fig. 4(b) is the same as that of a period-5 orbit of the uncoupled system except a small increase of the noise level.

The stabilized high-period orbits are not clearly shown in Fig. 2(a) because the stabilizing range of the driving voltage  $V_1$  is very narrow. High-period orbits are found to be a little more unstable than the low-period orbits

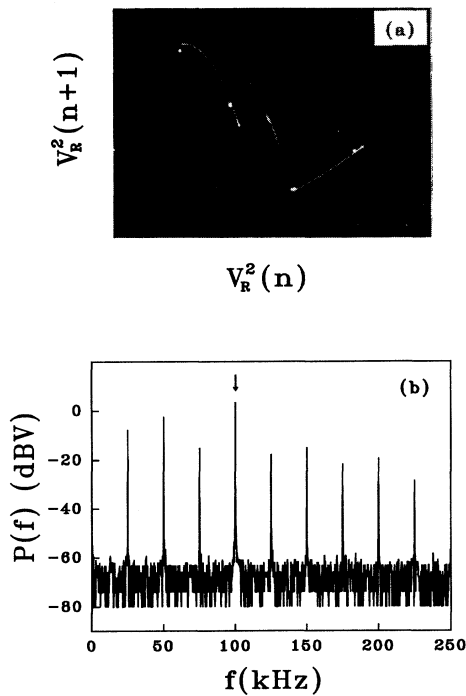


FIG. 3. (a) Double exposure showing the return map of the stabilized period-4 orbit at  $V_1=2.50$  V and  $V_2=4.25$  V (overexposed four dots) and the chaotic attractor. The vertical axis has arbitrary units. (b) A power spectrum of the stabilized orbit in (a).

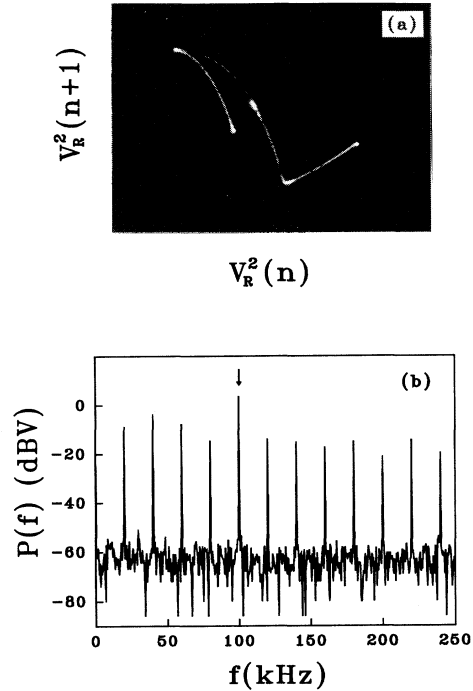


FIG. 4. The stabilized period-5 orbit at  $V_1=1.86$  V and  $V_2=4.25$  V. (a) A return map of the periodic orbit with the double-exposed chaotic attractor. The vertical axis has arbitrary units. (b) A corresponding power spectrum of the stabilized orbit.

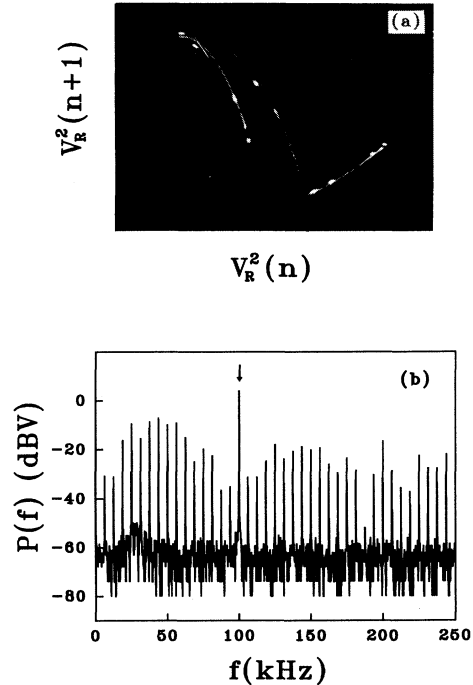


FIG. 5. Stabilized high-period orbits. The orbits are not clearly seen in Fig. 2(a). (a) Double exposure showing the return map of the period-9 orbit at  $V_1=4.98$  V and  $V_2=4.25$  V and the chaotic attractor. The vertical axis has arbitrary units. (b) A power spectrum of the period-16 orbit at  $V_1=3.40$  V and  $V_2=4.25$  V.

shown in Figs. 3(a) and 4(a), but it is not too difficult to identify such orbits by observing the return maps. Figure 5(a) shows a return map of the stabilized period-9 orbit at  $V_1=4.98$  V and  $V_2=4.25$  V with the chaotic attractor. Figure 5(b) is a power spectrum of the period-16 orbit at  $V_1=3.40$  V and  $V_2=4.25$  V. It is the highest-period orbit we have observed in the experiments. The orbits in Figs. 5(a) and 5(b) are new orbits which cannot be observed in the uncoupled diode resonator. Therefore the emergence of the additional periodic orbits by the weak coupling to the system in chaos is strong evidence that the chaotic attractor consists of an infinite number of unstable periodic orbits.

As we vary  $V_1$  of the drive system with  $V_2$  set at the same value, we observe that the same periodic orbits emerge many times. The orbits with the same period always have the same return map which consists of dots at exactly the same positions in phase space. This suggests that there are embedded unstable orbits which can be easily stabilized by the coupling signals. Chaotic attractors at lower  $V_2$  (around 1.80 V) also show the similar suppression of chaos by the weak coupling as that at  $V_2=4.25$  V. More periodic orbits are found by applying the same range of the coupling signals used for the attractor at 4.25 V. We find that it is harder to stabilize the attractor in a deep chaotic state ( $V_2=9.80$  V) but we can still see several low-period orbits at relatively higher  $V_1$ .

### III. DISCUSSION

Chaos in the driven diode resonator has been studied extensively by many authors [11–13]. The physical reason for chaos in the diode resonator is known as the nonlinearity of the diode capacitance with respect to the diode voltage [11,12] and the reverse recovery time of the diode [13]. Differential equations derived from the standard model of the  $p$ - $n$  junction diode [14] are found to give good qualitative agreements with the experimental results such as period-doubling and period-adding bifurcations [10].

Chaotic dynamics of strongly coupled diode resonators has been also studied [15,16]. Most of the routes to chaos for the strong coupling are quasiperiodic with various frequency lockings, which is not observed in our experiments. Using the model of the ideal  $p$ - $n$  junction diode we derive two linearly coupled differential equations with the assumption that the mutual inductance  $M$  of the coupling inductor is much smaller than the main inductance  $L$ . For the weak coupling the coupled equations are

$$\begin{aligned} \frac{d^2 Q_1}{dt^2} + \frac{1}{L} \left[ R + \frac{L}{C} \frac{\partial I_1}{\partial V_1} \right] \frac{dQ_1}{dt} + \frac{1}{L} (RI_1 + V_1) \\ - \frac{MR}{L^2} \frac{dQ_2}{dt} = \frac{V_1}{L} \sin(\omega t), \quad (1a) \end{aligned}$$

$$\begin{aligned} \frac{d^2 Q_2}{dt^2} + \frac{1}{L} \left[ R + \frac{L}{C} \frac{\partial I_2}{\partial V_2} \right] \frac{dQ_2}{dt} + \frac{1}{L} (RI_2 + V_2) \\ - \frac{MR}{L^2} \frac{dQ_1}{dt} = \frac{V_2}{L} \sin(\omega t), \quad (1b) \end{aligned}$$

where  $Q$ ,  $C$ ,  $I$ , and  $V$  are charge, capacitance, current, and voltage of the diode, respectively. Subscripts 1 and 2 represent the diode number in Fig. 1. We see that the linear coupling is made through the current via the mutual inductance  $M$ .

Coupled nonlinear maps have been studied theoretically by many authors for simplicity of computational work [17–20]. In particular the theoretical works on two linearly coupled logistic maps [17,18], which may be related to our work, have shown that there are regions in the system parameter space where the qualitative behavior of the coupled maps is quite different from that of the uncoupled logistic map. When complicated nonlinear systems such as the diode resonators are coupled to each other, we expect that things are much more complicated. The suppression of chaos by the weak coupling may be one of the things that have not been studied fully yet.

In our experiments we find that very small perturbations can change the chaotic dynamics drastically as in the recently proposed techniques of controlling chaos. While it is difficult to stabilize high-period orbits by using a feedback mechanism such as the OGY method, we have observed many stabilized high-period orbits by the weak coupling. When small and periodic coupling signals from the drive system are applied, the parametric amplification may make the chaotic dynamics regular such that weak periodic external forcing to the chaotic system eliminates chaos [5]. However, it is probably too early to speculate on the mechanism for stabilization of the high-period orbits from the chaotic attractor by the chaotic coupling signals.

To summarize, we have demonstrated experimentally that chaos of the diode resonator can be suppressed by the weak linear coupling to a system with the same dynamical property. The weak-coupling method is found to be efficient in reducing chaos even in a deep chaotic state into stable periodic motions but more careful study of the coupling effect on a chaotic attractor is needed to control chaos. Our experiments also support that a chaotic attractor consists of an infinite number of unstable periodic orbits.

### ACKNOWLEDGMENTS

We wish to thank S. Kim for helpful comments in the preparation of the present paper. Y. Kim thanks the Korea Science Foundation (Grant No. 923-0200-003-2) for support. S.-I. Kwun was supported in part by the Korea Science and Engineering Foundation through the Science Research Center of Excellence Program and the Basic Science Research Institute Program, Ministry of Education of Republic of Korea.

- [1] E. Ott, C. Grebogi, and J. A. Yorke, *Phys. Rev. Lett.* **64**, 1196 (1990).
- [2] W. L. Ditto, S. N. Rausso, and M. L. Spano, *Phys. Rev. Lett.* **65**, 3212 (1990).
- [3] J. Singer, Y.-Z. Wang, and Haim H. Bau, *Phys. Rev. Lett.* **66**, 1123 (1991).
- [4] D. Auerbach, C. Grebogi, E. Ott, and J. A. Yorke, *Phys. Rev. Lett.* **69**, 3479 (1992).
- [5] Y. Braiman and I. Goldhirsch, *Phys. Rev. Lett.* **66**, 2545 (1991).
- [6] K. Wiesenfeld and B. McNamara, *Phys. Rev. A* **33**, 629 (1986).
- [7] P. Bryant and K. Wiesenfeld, *Phys. Rev. A* **33**, 2525 (1986).
- [8] R. Lima and M. Pettini, *Phys. Rev. A* **41**, 726 (1990).
- [9] A. Azevedo and S. M. Rezende, *Phys. Rev. Lett.* **66**, 1342 (1991).
- [10] S. D. Boron, D. Dewey, and P. S. Linsay, *Phys. Rev. A* **28**, 1201 (1983).
- [11] P. Linsay, *Phys. Rev. Lett.* **47**, 1349 (1981).
- [12] J. Testa, J. Pérez, and C. Jeffries, *Phys. Rev. Lett.* **48**, 714 (1982).
- [13] R. W. Rollins and E. R. Hunt, *Phys. Rev. Lett.* **49**, 1295 (1982).
- [14] *Electronic Designer's Handbook*, edited by L. J. Giacoletto (McGraw-Hill, New York, 1977).
- [15] R. B. Birs Kirk and C. Jeffries, *Phys. Rev. A* **31**, 3332 (1985).
- [16] Z. Su, R. W. Rollins, and E. R. Hunt, *Phys. Rev. A* **40**, 2689 (1989).
- [17] J.-M. Yuan, M. Tung, D. H. Feng, and L. M. Narducci, *Phys. Rev. A* **28**, 1662 (1983).
- [18] K. Kaneko, *Prog. Theor. Phys.* **69**, 1427 (1983).
- [19] T. Hogg and B. A. Huberman, *Phys. Rev. A* **29**, 275 (1984).
- [20] H. Kook, F. H. Ling, and G. Schmidt, *Phys. Rev. A* **43**, 2700 (1991).

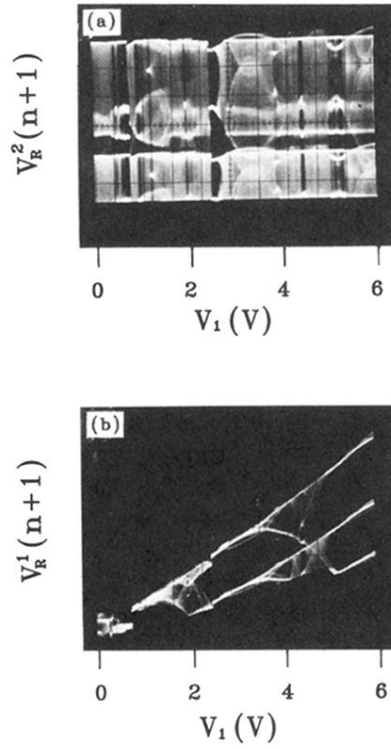


FIG. 2. (a) A bifurcation diagram showing the change of chaos of the response system at  $V_2 = 4.25$  V as a function of  $V_1$  of the drive system.  $V_1$  is varied from 0 to 6.0 V. Note that various periodic orbits from the chaotic attractor are emerged in several regions of  $V_1$ . Arbitrary units are used for the vertical axis. (b) A bifurcation diagram of the drive system for the same range of  $V_1$  ( $V_2 = 4.25$  V). Because of the weak coupling the diagram is very similar to that of the uncoupled resonator. Arbitrary units are used for the vertical axis.